UTEC 76-127

SQ

(NASA-CR-150031) PREPARATION AND CHARACTERIZATION OF METHACRYLATE HYDROGELS FOR ZETA POTENTIAL CONTROL Final Report (Utah Univ.) 51 p HC A04/MF A01 CSCL 07D

N77-10166

Unclas

G3/25 09635

FINAL REPORT

NATIONAL AERONAUTICS AND SPACE ADMINISTRATION

Contract NAS 8-~~3023~~
30253

PREPARATION AND CHARACTERIZATION OF METHACRYLATE HYDROGELS FOR ZETA POTENTIAL CONTROL

by

D. E. Gregonis, S. M. Ma, R. Van Wagenen
and J. D. Andrade
Department of Materials Science and Engineering
University of Utah
Salt Lake City, Utah 84112

to

Dr. J. Patterson, Contract Monitor
National Aeronautics and Space Administration
Marshall Space Flight Center
Alabama 35812

February 15, 1976

NOV 1976
RECEIVED
NASA STI FACILITY
INPUT BRANCH

TABLE OF CONTENTS

I. SUMMARY/ABSTRACT

A technique based on the measurement of streaming potentials has been developed to evaluate the effects of hydrophilic coatings on electroosmotic flow. The apparatus and procedure are described as well as some results concerning the electrokinetic (ζ) potential of glass capillaries as a function of ionic strength, pH, and temperature. The effect that turbulence and entrance flow conditions have on accurate streaming potential measurements is discussed. Various silane adhesion promoters exhibited only a slight decrease in streaming potential. A coating utilizing a glycidoxy silane base upon which methylcellulose is applied affords a six-fold decrease over uncoated tubes. Hydrophilic methacrylate gels show similar streaming potential behavior, independent of the water content of the gel. By introduction of positive or negative groups into the hydrophilic methacrylate gels, a range of streaming potential values are obtained having absolute positive or negative signs.

II. BACKGROUND/RATIONALE

This work has been conducted to support the free zone cell electrophoresis experiment performed during the Apollo-Soyuz flight in July, 1975. In this experiment the electrophoresis apparatus utilized pyrex tubes which functioned as the cell electrophoresis chamber. These tubes were split in half, lengthwise, and then rejoined using RTV silicone to seal the seams, reforming the tube for better thermo-stress stability. For the experiment the tube contained aqueous buffer solution and a zone of cells. When a potential is applied at the ends of the tube, the cells migrate in the buffer according to the charge associated with the particular cell.

Pyrex glass, however, has a negative electrical charge associated with its surface due to silanol and boranol groups at the glass surface. The counter-ions to these surface charges are free to migrate in the electric field resulting in a back flow of charge along the surface. This phenomenon is called electroosmosis and results in an unequal migration of the cells characterized by a parabolic-shaped flow profile. Since a uniform cell migration is highly desired, a modification of the pyrex glass surface is necessary to decrease or eliminate electroosmosis. This can be done by either neutralization of the glass surface charge or by coating the surface with a polymer to mask the charge.

This report describes and evaluates surface coatings for reducing or eliminating electroosmosis. We used the streaming potential method to evaluate the surfaces prepared. The determinations are made by flowing an electrolyte, usually an aqueous buffer, through a capillary tube and measuring the potential generated between the ends of the capillary. This potential is called the streaming potential and results because part of the counter ion layer associated with the surface is carried along with the flowing electrolyte.

The first half of this report describes the design of the streaming potential apparatus, the variables involved in streaming potential measurement and the experimental protocol. The second half of this report describes surface modifications of the pyrex glass and its effect on streaming potential. The surface modifications can be further divided into: 1) Silane surface treatments, 2) Polysaccharide surface treatments, and 3) Hydrophilic synthetic polymer surface treatments.

III. DEVELOPMENT OF STREAMING POTENTIAL APPARATUS AND PROTOCOL

A. Introduction

The initial objective of this research was to develop an apparatus and experimental technique which could directly measure the electrokinetic properties of capillary surfaces. The approach chosen was based on the streaming potential phenomena orginally quantitated by Helmholtz and Smoluchowski (1) and explained in some detail by Davies and Rideal (2).

The relationship between the measured streaming potential and the potential at the hydrodynamic shear plane, the zeta (ζ)-potential, is given as

$$(1) \qquad \zeta = \frac{4\Pi\eta}{\varepsilon} \frac{Estr}{P} \left[K_B + \frac{2Ks}{a} \right] ,$$

where η and ε are viscosity and dielectric constant, respectively, in the diffuse double layer, Estr is the streaming potential measured across the streaming capillary, P is the pressure difference across the capillary responsible for the flow of electrolyte, a is the radius of the capillary, and K_B and K_s are the specific bulk and surface conductivities. The zeta potential, ζ, can be calculated from measurements of streaming potential and driving pressure if surface conductance is taken into account. This is accomplished by utilizing Equation 2:

$$(2) \qquad \zeta = \frac{4\Pi\eta}{\varepsilon} \frac{Estr}{P} \frac{C}{R} \quad \text{, where}$$

C is the predetermined system constant and R is the measured a.c. resistance of the capillary-electrolyte system.

Normally Equation 2 is utilized when ionic strength is so low that surface conductance comprises a significant proportion of the total conductance. At high ionic strengths, i.e., physiological electrolyte concentrations, surface conductance is negligible compared to the total conductance, and Equation 1 simplifies to Equation 3:

$$(3) \qquad \zeta = \frac{4\Pi\eta\, K_B}{\varepsilon} \quad \frac{Estr}{P} \quad .$$

K_B can then be determined in a standard conductivity cell utilizing platinized gray platinum electrodes. Viscosity and dielectric constant in the diffuse layer are assumed to be equal to bulk values; however, this is probably incorrect according to Haydon (3).

Ball and Fuerstenau (4) have reviewed the streaming potential literature in regard to Estr/P data. They have concluded that, due to as yet unexplained flow and asymmetry potentials common to a wide variety of electrode types, the slope of the loci of Estr data at a number of driving pressures in opposite flow directions (ΔEstr/ΔP) should be utilized in Equations 1, 2, and 3. This has been the case in this research where the loci of streaming potential data as a function of driving pressure in both flow directions has been fitted to a linear regression best fit straight line using a Hewlett Packard (Model 9820A) programable calculator.

B. Apparatus

The streaming potential apparatus is illustrated in Figure 1. It is composed entirely of borosilicate (Corning 7740) glass with the exception of two sections of Silastic (Dow Corning, poly(dimethyl siloxane), medical grade) tubing (F) used to connect the streaming capillary (E) to the electrode chambers (C). The electrodes are of the silver, silver chloride type and are prepared by the anodic electrolytic deposition of an AgCl coating on a silver wire (A. D. MacKay, N. Y.). The wire electrodes are in the form of a spiral and are epoxied into 7/15 $\mathrm{\Xi}$ glass joints which mate with the electrode chambers. Two 200 ml reservoirs (A) serve as containers

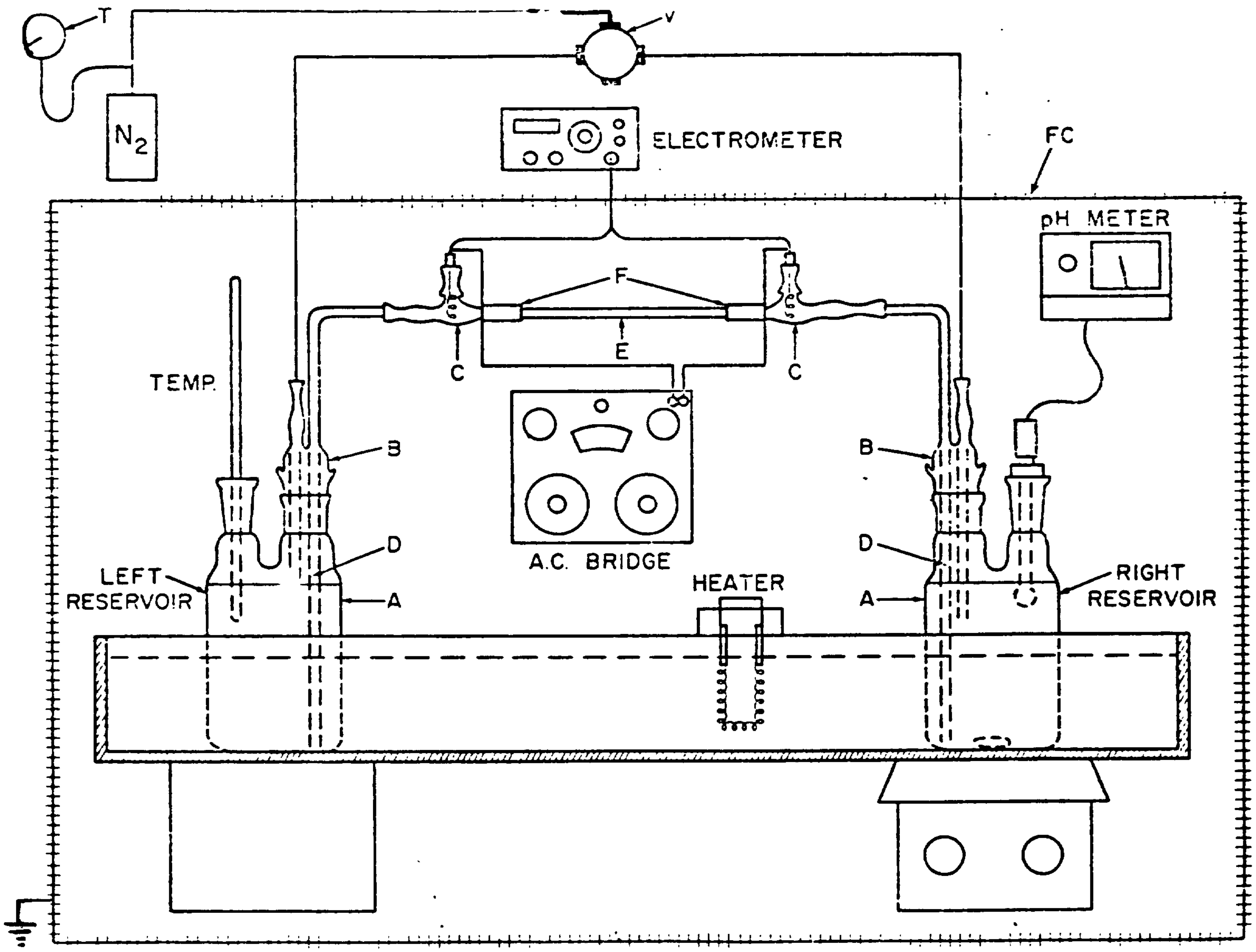

Figure 1. The Streaming Potential Apparatus. Refer to text for description.

for the streaming fluid and are connected to the electrode chambers (C) and an N_2 pressure source via Section B. Section D is a dip tube extending to the bottom of each reservoir. Sections A, B, C, and D are connected together via 7/15 and 19/22 $\$$ glass joints and were made small enough to be radio frequency glow discharged prior to each streaming experiment.

The reservoirs are positioned in a constant temperature bath and stirring can be accomplished with a magnetic stirrer. The system pH (Corning Model 12 pH meter and glass electrode combination) and temperature (0-100°C, accurate to ± 1°C) can be monitored continuously. Purified N_2 gas (99.999% pure) serves as a pressure source utilized to drive the streaming fluid through the capillary. The four-way ball valve (V) (Whitey Model B-43YF2) simultaneously exposes one reservoir to N_2 driving pressure and the other to atmospheric pressure. A 90° rotation of the valve applies pressure to the opposite reservoir and reverses the electrolyte flow. Pressure is adjusted with a two-stage oxygen regulator (Matheson Gas Products Model 3104) with an adaptor for N_2 and a Tycos pressure gauge (T) (0-300 mm Hg, accurate to 1 mm Hg). The components of the pressure drive system are connected to the streaming apparatus via Silastic tubing. The streaming potential is measured with a high input impedance digital electrometer (Keithley Model 616), and the resistance of conductance of the streaming fluid is measured with an a.c. bridge at a frequency of 1KHz (General Radio Model 1650B). The streaming apparatus is electrically isolated from extraneous electrical signals by a Faraday cage (copper screen 50 mesh/inch) (FC).

C. Procedure

Streaming potential data was obtained by measuring streaming potentials at a driving pressure of 2 cm Hg, then reversing the flow direction and repeating the measurement. The driving pressure was increased by 2 cm Hg and streaming potentials were again measured in both flow directions. This process was repeated until the driving pressure reached 12 to 14 cm Hg. The slope, $\Delta E_{str}/\Delta P$, of the best fit straight line was utilized in Equation 3. Solution specific conductivities were determined in a precalibrated cell with platinized platinum electrodes. The cell constant, C, of the streaming capillary and the conductivity cell were predetermined using a .1 N KCl solution of known specific conductivity (5). Following streaming measurements, the resistance of the capillary electrode system was measured with the a.c. bridge. In most instances where ionic strength was high, solution conductivities masked surface conductivities and κ_B could be determined in a conventional conductivity cell. Equation 3 was then utilized. This was the case for all data reported here.

Radio frequency glow discharge (RFGD) cleaning of the streaming cell components was carried out to eliminate problems with surface contamination which occasionally developed. RFGD (commercial Plasmod system, Tegal Corporation, Richmond, California) in argon gas at 100 μmHg and an RF power density of 50 watts for 5 minutes was highly effective in removing surface contamination.

Water used in this study was twice distilled over Pyrex Glass (Corning Still Model AG-11) and had a conductivity of 1 ± .1 umho/cm. Phosphate buffered saline (PBS) was made up as .145 M NaCl, 2×10^{-4} M KH_2PO_4, and 8×10^{-4} M Na_2HPO_4 using twice distilled water. For the evaluation of silane and polymer coatings in part IV, a potassium chloride buffer was used containing 0.01 M KCl, 2×10^{-4} M KH_2PO_4, 8×10^{-4} M Na_2HPO_4. The pH measured 7.2 ± 0.1.

D. Results and Discussion

1. Tube dimensions.

Preliminary investigations concerning the effect of capillary geometry on measured streaming potential indicated a linear decrease in ΔEstr/ΔP as the length of the capillary decreased. This was at odds with the conclusion inherent in the derivation of the streaming potential equation in that capillary geometry should not affect the streaming potential. An analysis of flow turbulence and entrance effects on streaming potential was carried out to determine the cause of the discrepancy.

Figure 2 is an Estr vs. P plot for two streaming tubes. Tube A is 600 μm I. D. and 30 cm in length, while Tube B is 1250 μm I. D. and 30 cm long. In the case of Tube A the data is linear and the slope (ΔEstr vs. ΔP) is equal in both flow directions. Measured flow rates and subsequently calculated Reynolds numbers indicated laminar flow throughout the measured pressure range for Tube A. In the case of the larger tube (B), the data at low driving pressures is linear and the slopes are equal in both flow directions; however, at a pressure of 14 cm Hg the flow becomes turbulent ($R>2000$) and the data becomes nonlinear at higher driving pressures. This seems to indicate a marked deviation in the ΔEstr/ΔP data obtained if the flow changes from laminar to turbulent. This is at odds with data published by others (5) for turbulent flow in aqueous systems. One can also see a difference in ΔEstr/ΔP for Tubes A and B which would seem to indicate that turbulent flow is not the only cause of deviations in the calculated ζ-potential for tubes of various sizes.

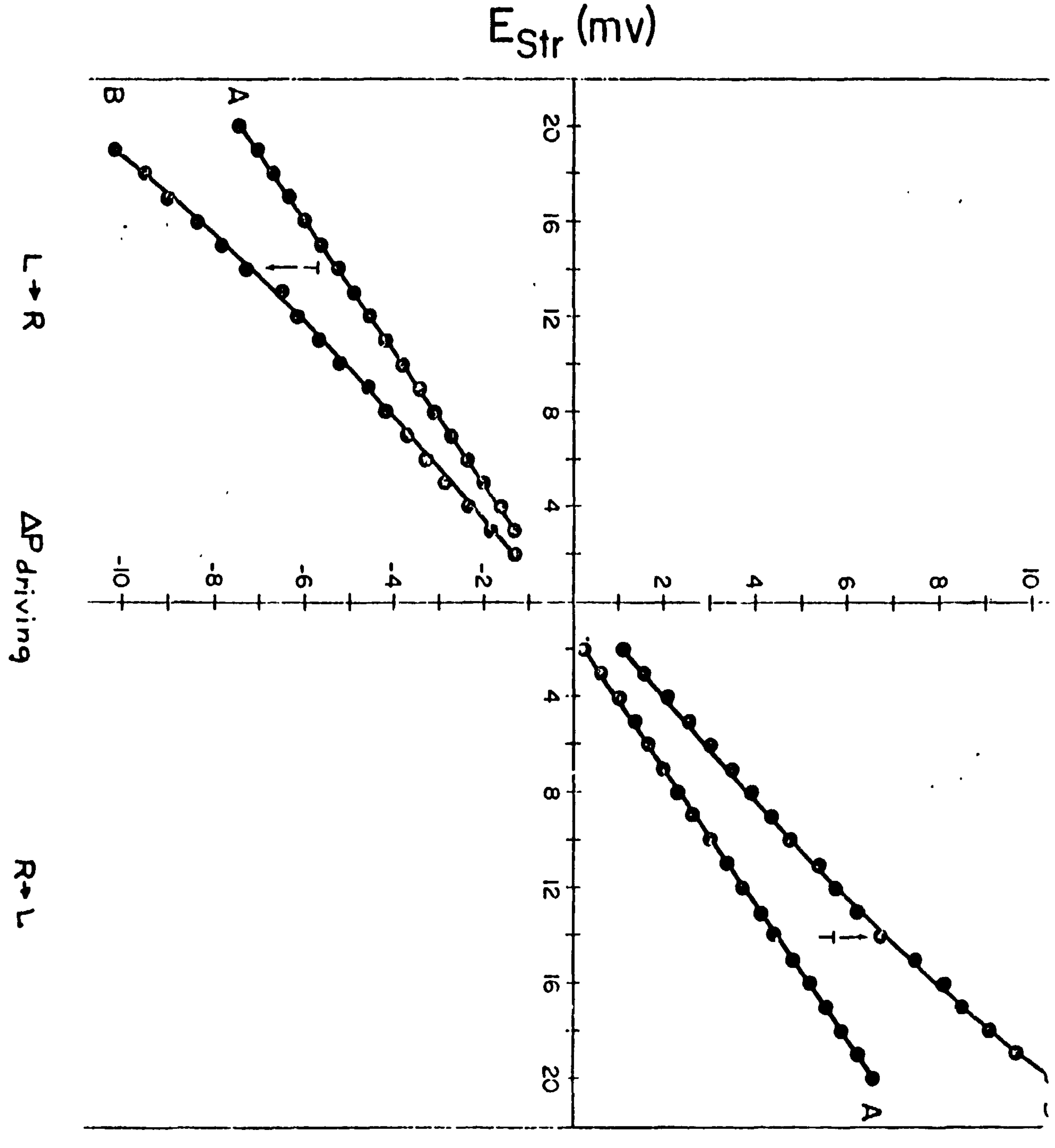

Figure 2. ΔEstr/ΔP plot for 2 capillaries. Tube A is 600 µm I.D. and 30 cm long; Tube B is 1250 µm I.D. and 30 cm long. Refer to t-xt for discussion.

The results of streaming potential studies on borosilicate capillaries as a function of length and internal diameter are shown in Figure 3. Each tube was evaluated at its greatest length and then successive portions were removed and it was reevaluated. This was continued until no tube remained. The only variable was $\Delta Estr/\Delta P$ since η and ε are assumed constant and K_B greatly predominated over K_S at this high ionic strength (.01 gm ions/L). Capillaries B (1284 ± 34 μm I. D.) and C (595 ± 15 μm I. D.) were commercial borosilicate (pyrex); there was no significant variation in I. D. along the length. Both capillaries exhibited a constant $\Delta Estr/\Delta P$ value until a critical length was reached where-upon there was a marked drop in $\Delta Estr/\Delta P$. The critical length (L_e) at which this occurred was 58 cm for Tube B and 20 cm for Tube C. Capillary A was hand drawn for a larger tube. There were significant variations in I. D. along its length. Points 1 and 2 shown in Figure 3 were obtained when the capillary was 190 ± 12 μm I. D., while equivalent lengths taken from the center of the tube gave lower $\Delta Estr/\Delta P$ values and had an I. D. of 160 ± 5 μm. This would seem to indicate that at lengths less than some critical length the diameter of the streaming capillary markedly affects the measured streaming potential, while at lengths greater than L_e minor variations in diameter have no measurable effect.

The onset of turbulent flow does not seem to cause this behavior since flow was laminar in all cases for Tubes A and C and there seemed to be no significant effect due to turbulent flow for Tube B. If one compares the measured flow rates, Q_m, in the three tubes with the theoretical flow rates, Q_t, calculated using Poiseuille's law as expressed in Equation 4,

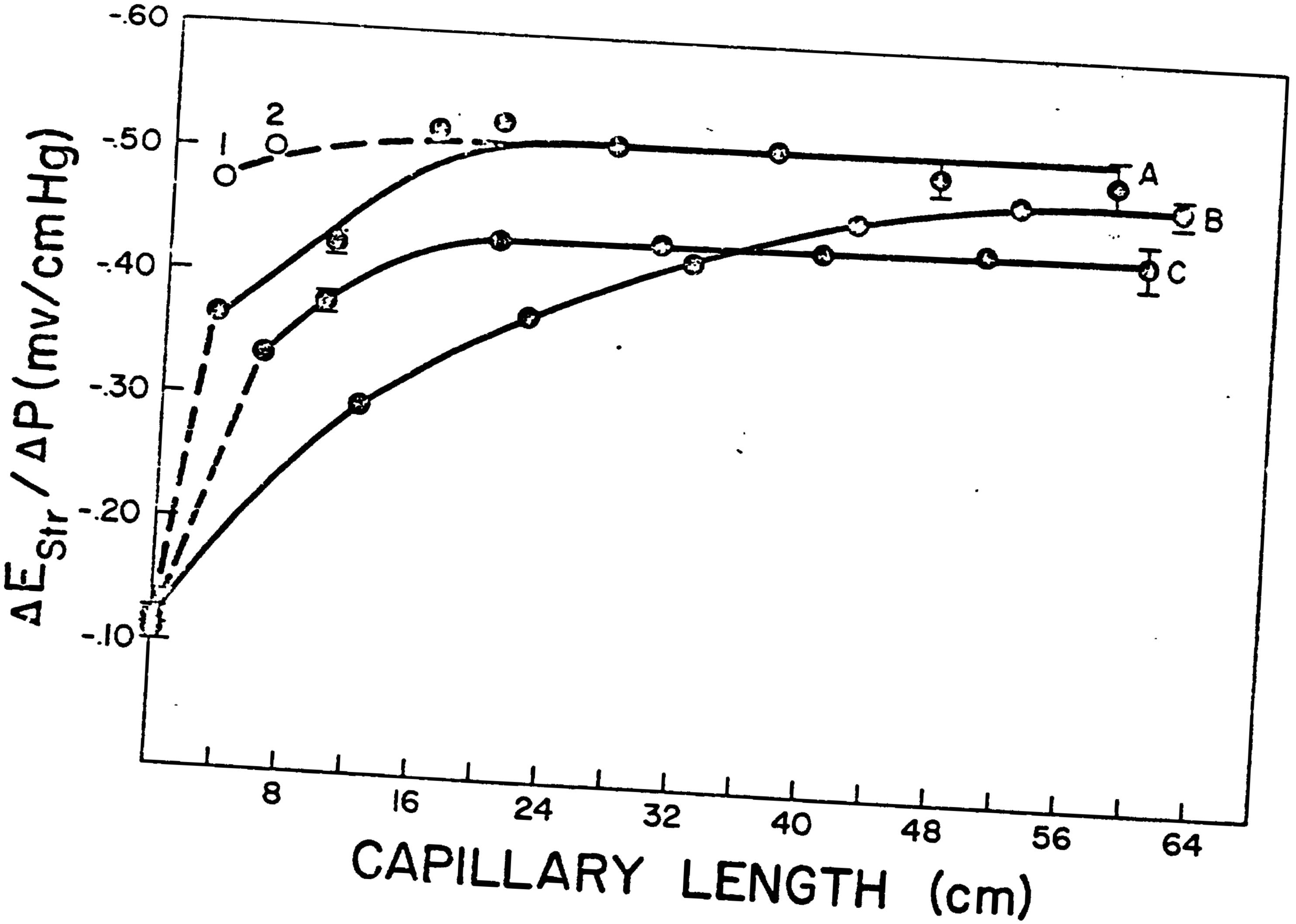

Figure 3. ΔEstr/ΔP as a function of capillary length. B. 1284 μm I.D.; C. 595 μm I.D. Refer to text for complete discussion.

$$(4) \qquad Q_t = \frac{\pi}{8} \frac{r^4}{\eta} \frac{dP}{dx} ,$$

where r is the tube radius, η is the fluid viscosity, and dP is the pressure drop across the flow length dX, it is found that Q_t and Q_m are equal until the critical length, L_e, is reached, i.e., 20 cm for Tube C and 58 cm for Tube B. It can be concluded from this that the streaming data and calculated zeta potential are independent of capillary geometry (the variation in plateau values of $\Delta Estr/\Delta P$ are expected since the tubes were from different sources and most probably had different surface histories) as long as Poiseuille flow exists. This is what Helmholtz predicted as Bocquet has pointed out (6). Poiseuille flow actually requires that four basic conditions exist, i.e., the flow is steady, incompressible, laminar, and established.

Many investigators have simply ignored the established flow criteria. It takes a certain length, L_e, past the entrance of a cylindrical flow system, to establish a parabolic velocity profile during steady laminar flow of an incompressible fluid. The value of L_e has been found both experimentally (7) and theoretically (8) to be given by Equation 5.

$$(5) \qquad L_e \approx 0.06\, RD,$$

where R is the Reynolds number, and D is the diameter. On the basis of this analysis, it seems that if L_e is greater than 10 ± 1% of the total streaming tube length, the $\Delta Estr/\Delta P$ ratio and subsequently calculated ζ-potential will be anomalously low.

2. Electrodes

Electrode asymmetry at high ionic strength can develop, particularly if the electrodes have aged appreciably over the course of several month's use, and if they have been exposed to protein or other adsorbable solutes. Since other experiments in our lab utilized the streaming potential apparatus for biological evaluation (9), the effects of these experiments on the silver, silver chloride electrodes had to be taken into account. This is illustrated in Figure 4. Curves 8B through 12B were obtained utilizing silver, silver chloride electrodes which had previously been exposed to a streaming capillary with a surface of adsorbed fetal calf serum. The asymmetry developed at that time. It was absent in earlier experiments at high ionic strength (.1 gm ions/L) where protein was not present (not shown). The asymmetry diminished with continuous streaming of electrolyte in approximately 30 minutes (8B to 10B). As long as streaming continued, the slope ΔEstr/ΔP (10B to 12B) remained constant. If flow ceased for any length of time, asymmetry reappeared and it required another 30 to 40 minutes of streaming to obtain good linearity and reproducibility. At lower ionic strength (.01 gm ions/L) the asymmetry was not evident (1B and 4B, Figure 4). When fresh electrodes were prepared and protein contanimation was absent, there was no deviation from linearity at low ionic strength (.01 gm ions/L) or high ionic strength (.1 gm ions/L).

The asymmetry exhibited by aged silver, silver chloride electrodes at high ionic strength may be due to protein adsorption in the pores of the AgCl coating. Janz and Ives (10) maintain that silver may form stable complexes with animo and sulfhydryl groups of organic molecules which can compete with the insolubility of the AgCl thus negating the proper functioning of the electrodes. It has also been suggested (10) that 10-25% of the silver should be chloridized to AgCl to produce electrodes having good reproducibility and stability. The electrodes exhibiting asymmetry problems had only 1% conversion (assuming 100% current efficiency) of Ag to AgCl. Srinivasan (11) has recommended that silver, silver chloride electrodes be prepared in a slowly alternating a.c. fashion utilizing anodic

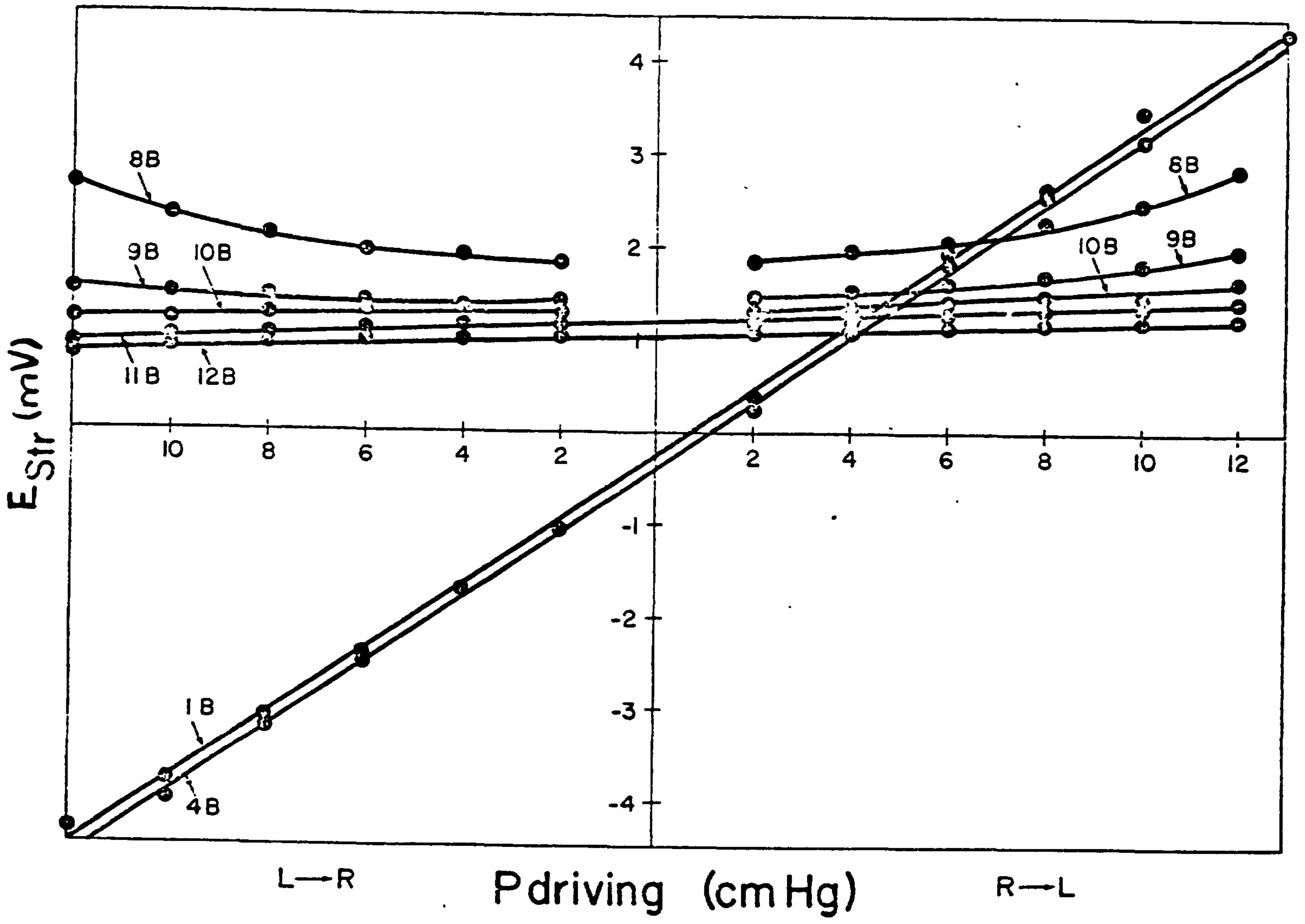

Figure 4. Effect of electrode asymmetry on ΔEstr. See text for discussion.

deposition of AgCl and cathodic current to decrease surface area by enhanced pore formation. The above recommendations were followed. Silver, silver chloride electrodes were prepared electrolytically with a slow alternating current (5 minute anodic, 2 minute cathodic, etc.); the gross surface area per electrode was 1 cm^2 and the net anodic current density time produced was 6.9 amp sec/cm^2. There was a theoretical conversion of silver to silver chloride of 16%. Electrodes freshly prepared in this fashion are stable and have never shown prolonged asymmetry at high ionic strength even upon protein adsorption.

Figure 5 comprises four scanning electron micrographs (SEM) of silver, silver chloride electrode surfaces. The general shape of the electrodes used in this study are shown in Figure 5a. They consist of silver wire coils 6 mm long and 3.8 mm O. D. The gross surface area is 1 cm^2. Figure 5b illustrates the AgCl surface of a freshly prepared electrode (anodic 5 ma/cm^2 for 4 min, 1% conversion of Ag to AgCl). A number of pores can be seen as well as some microgranularity on a cobblestone surface. Figure 5c is the same electrode after approximately 3 months use. This was the same electrode which developed asymmetry at high ionic strength and protein exposure. The cobblestone appearance is still partially evident; however, much of the pore structure and all of the micro texture are lost. The pores between the cobblestones are now replaced by smaller pores in an incomplete cobblestone structure. Figure 5d is the surface of a freshly prepared electrode employing the alternating anodic and cathodic deposition of AgCl previously described. The highly porous structure obviously increases the surface area available for current transport. Electrodes prepared in this manner have not exhibited asymmetry at high ionic strength and exposure to protein solutions as long as they are equilibrated several hours prior to use.

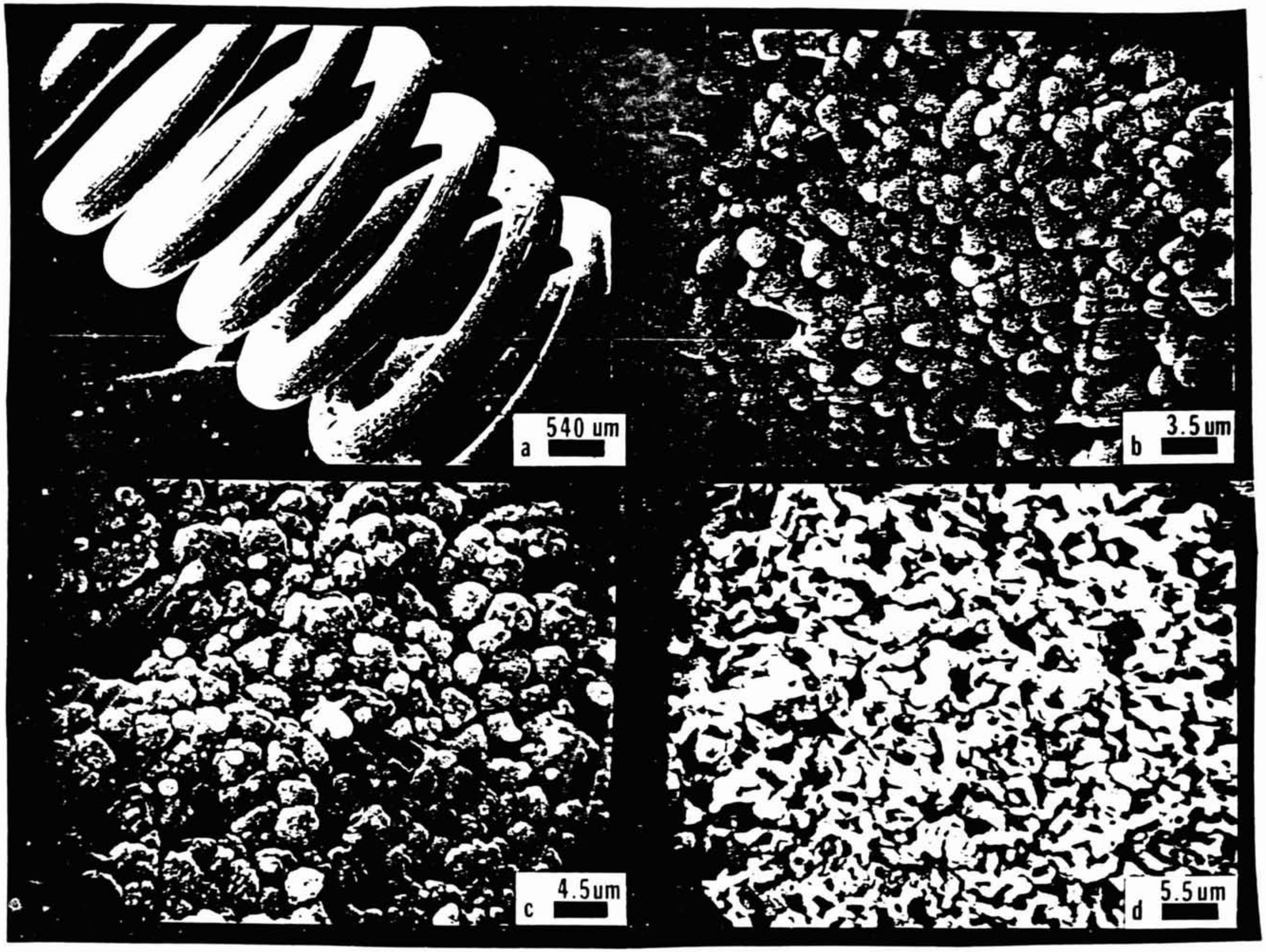

Figure 5. Scanning electron micrographs of silver/silver chloride electrode surfaces. See text for discussion.

3. Glass surfaces

The calculated zeta potential of borosilicate (pyrex) glass as a function of temperature indicated that there is no statistically significant variation in ζ-potential as a function of temperature, at least in 0.1 M NaCl solution.

The variation in zeta-potential with pH for borosilicate glass is shown in Figure 6. The data indicates that borosilicate has a pKa of ≃ 5.7 assuming that all the surface charge is due to the ionization of ionogenic ≡ Si-OH (silanol) groups in the hydrated region of the glass. This is at variance with the data of Hair and Hertl (12) and Marshall <u>et.al</u>. (13) which suggests a pKa for surface silanol groups of 7.1 to 7.2. However, it is quite probable that high concentrations of hydronium ions exist in the hydrated surface region of the glass due to cation exchange. If this were the case, the ζ-potential at acidic pH could be considerably less than that occurring as a result of charge generation purely by ionogenic silanol groups. The result would be an apparent shift in pKa. A second cause of the discrepancy may be due to the presence of boranol groups (≡ B-OH) in significant numbers at the hydrated surface of borosilicate glass. The proportion of boron to silicon in the porous surface may be as high as 1:3 rather than 1:18 as expected in the bulk (14). The pKa of boranol groups is 5.1 and this would also tend to shift the resultant surface pKa to a more acidic region.

Figure 7 illustrates the increase in ζ-potential with decreasing ionic strength (KCl) at constant pH (7.1) and temperature (26°C). The linear portion of the curve corresponds to the expansion of the electrical double layer as ionic strenth decreases. At an ionic strength of less than

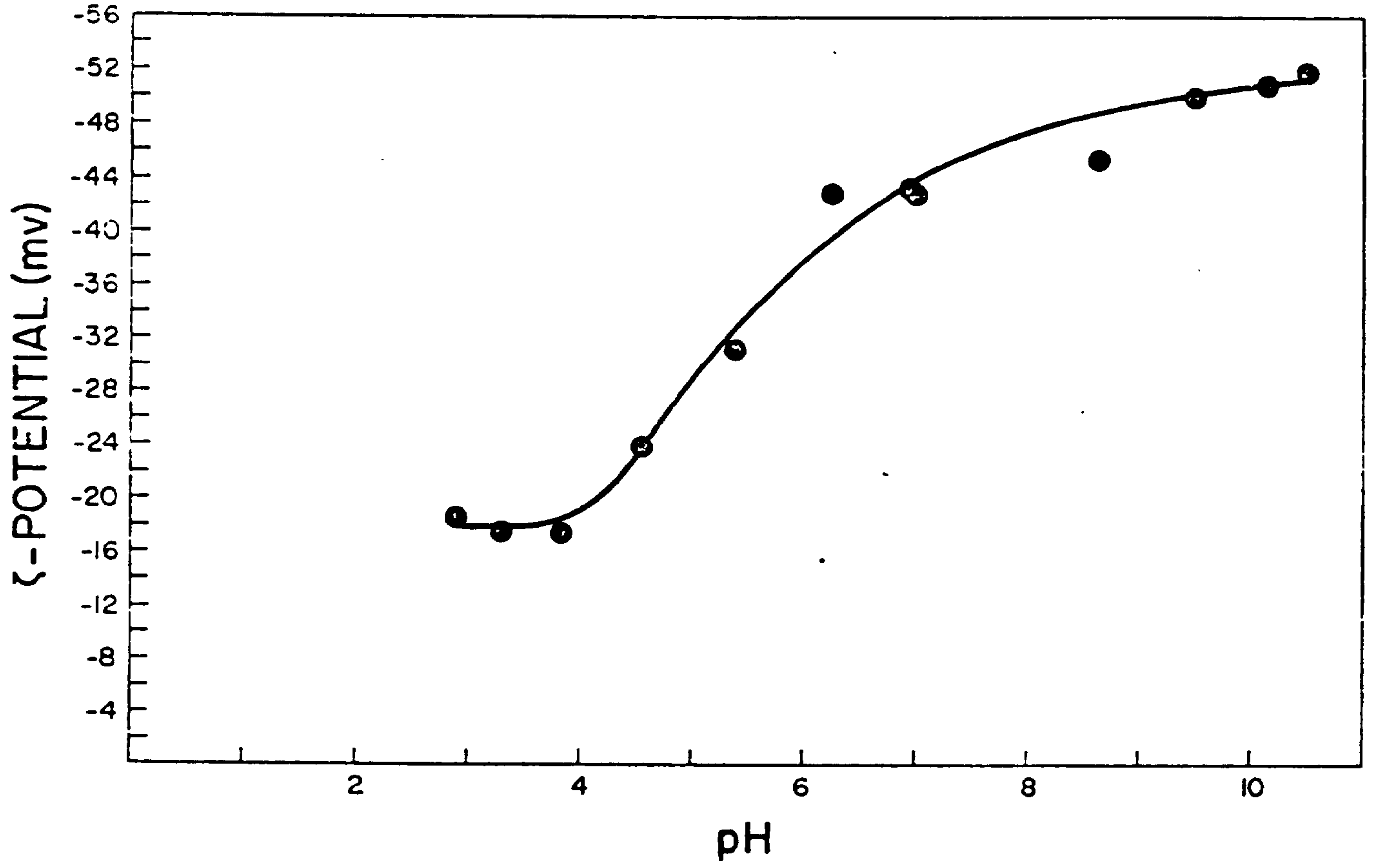

Figure 6. Calculated zeta potential from ΔEstr/ΔP data for borosilicate glass as a function of pH. See text for details.

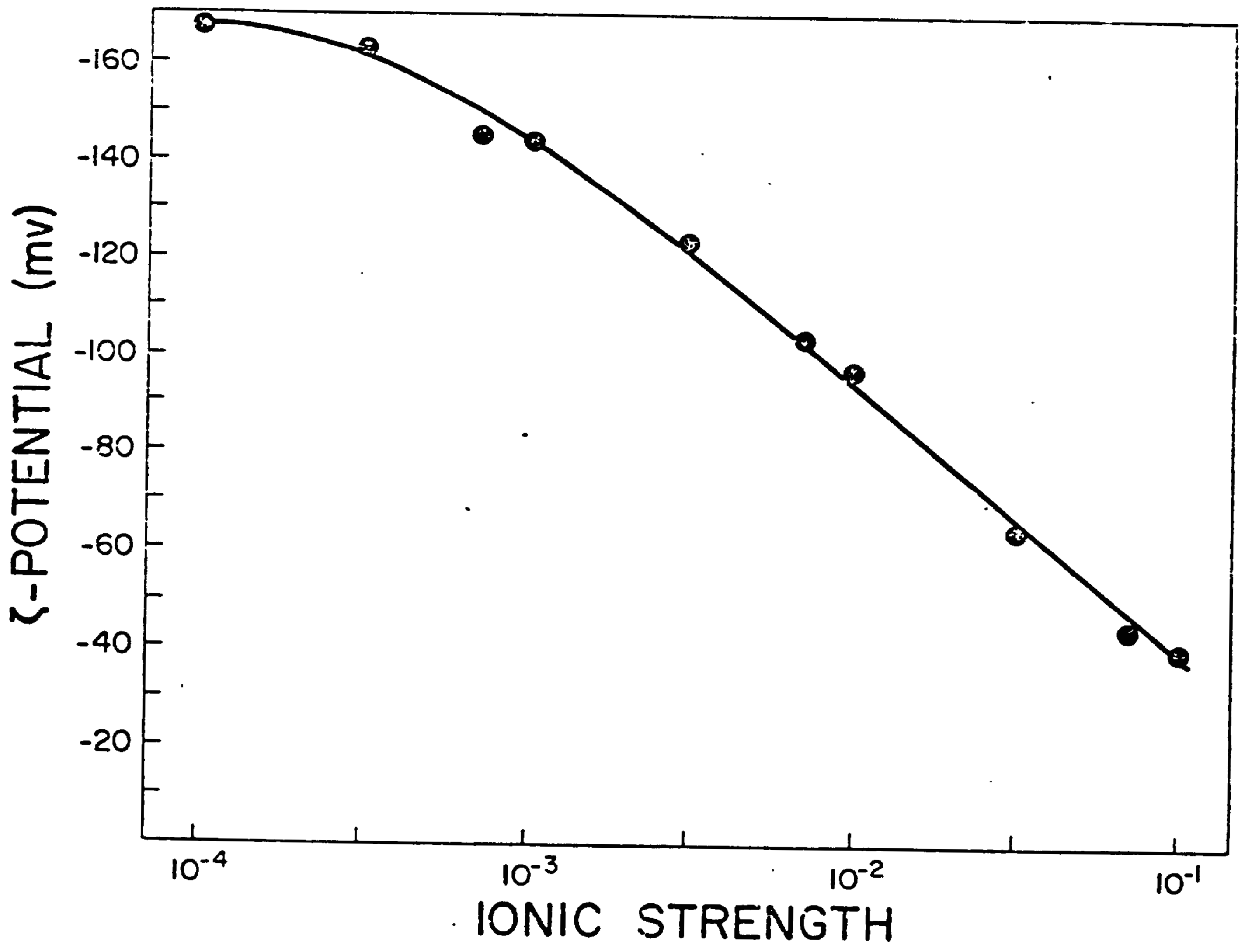

Figure 7. Effect of ionic strength on zeta potential of borosilicate glass at constant temperature (28°C) and pH (7.1).

3×10^{-4} gm ions/L there is a deviation from linearity due to the onset of surface conductance which was not accounted for in the calculation of ζ. This is in agreement with the detailed analysis of surface conductance made by Rutgers and DeSmet (15) and Li and deBruyn (16).

IV. EFFECTS OF VARIOUS COATINGS UPON STREAMING POTENTIAL

A. Background

For the analysis of various silane adhesion promoters and hydrophilic gels, commercially available, pyrex, thick-walled capillaries (Corning Glass Works, Corning, N.Y., 14830) were used. These tubes had the following dimensions: 0.1 mm I. D., 5-6 mm O. D. 150 mm long). The tubes were radio-frequency glow discharge cleaned before use. All tubes were measured three times, unless reported otherwise. The clean, uncoated tubes had streaming potential measurements (ΔEstr/ΔP) of -0.357 (tubes 1, 2, 3).

B. Effect of Silane Coatings

A wide variety of silanizing reagents were investigated to determine their effect on ΔEstr/ΔP values on glass surfaces. It has been reported that 1,1,1,3,3,3-hexamethyldisilazine (17) is a more reactive silanizing reagent than trimethylchlorosilane, because it is able to react with more hindered silanol groups on the glass surface to form trimethylsilane derivatives (18). To test if either of these silanizing reagents affect the streaming potential, several of the mounted tubes were silanized by the following procedure:

The silane is mixed with an equal volume of triethylamine. The solution is rinsed through the tube, first in one direction, then in the opposite direction. The tubes are then placed in vacuum at 120°C overnight.

Tubes 4, 5, 6 and 7 were coated with 1,1,1,3,3,3-hexamethyldisilazine. Tubes 8, 9, 10 and 11 were treated with trimethylchlorosilane. The average ΔEstr/ΔP of the 1,1,1,3,3,3-hexamethyldisilazine coated tubes is -0.242. The average of the trimethylchlorosilane tubes is -0.221. No significant difference is noted between these two silanizing reagents.

Three other silanizing reagents were investigated for their effect on ΔEstr/ΔP values on the capillaries: dimethyldichlorosilane (17) (Tube 12), γ-methacryloxypropyltrimethoxysilane (19) (Tube 13) and γ-glycidoxypropyltrimethoxysilane (19) (Tube 14). The silanizing procedure used is as described above using triethylamine as catalyst. Only tube 14 shows any substantial decrease in streaming potential. A tube repeating the exact coating proceedure used on Tube 14 was prepared (Tube 15), and this time the ΔEstr/ΔP values was typical of that obtained with all the silanizing reagents.

For trimethoxyalkylsilanes the literature reports contradictory data for the preferred procedure for silanization of glass surfaces. One group reports (20) better silanization occurs with n-propylamine catalyst. Another report (21) states silanization occurs best in pH 4 aqueous solution. We feel that the silanization process should be either acid or base catalyzed and used triethylamine, a stronger nitrogen base than n-propylamine, as a control. As judged from the streaming potential results in Tube 15, 16 and 17, no difference in ΔE/ΔP is found using the three different catalysts for γ-glycidoxypropyltrimethoxysilane (19). Triethylamine was used as catalyst for the remainder of the silane treatment.

C. Effects of Polysaccharide Coatings

γ-glycidoxypropyltrimethoxysilane was the silane selected upon which various polysaccharides were covalently attached. Standard solutions of various polysaccharides were prepared. The polysaccharide was dissolved in either 0.5% HCl or 0.5% KOH. If the polysaccharide forms a viscous solution, the viscosity was regulated by addition of the polysaccharide to the solution until it had the consistancy of thick syrup. Otherwise the polysaccharide was added to complete saturation. A water aspirator was placed on one end of the tube, and the polysaccharide solution was pulled through the tube. The aspirator was changed to the other end of the tube, and the polysaccharide solution was pulled through in the opposite direction. The tubes were placed in vacuum at 120°C for curing, unless otherwise specified. Finally, the tubes were exhaustively rinsed with distilled water before they were measured.

Methylcellulose (Dow Methocel MC, premium, 4000 cps), hydroxypropylmethylcellulose (Dow Methocel 90H6, premium, 15000 cps), dextrin (JAGUAR (hydroxyethyl guar HE-L) (23) and agarose (24), were the polysaccharides investigated. In this study, the methylcellulose/acid treatment or hydroxypropylmethylcellulose/acid treatment was obviously superior. Tube 22, which was treated with dextrin in 0.5% KOH, exhibited a fairly low value for streaming potential, but a duplicate experiment did not reproduce this observation (Tube 31). To see if a thicker polysaccharide coating would lower the ΔEstr/ΔP values, these tubes were treated with a polysaccharide containing either formaldehyde or 1,2,4,5,9,10-triepoxydecane (25) as crosslinker. The tubes were then cured in vacuum at 100° overnight. Although the ΔEstr/ΔP values were low, they showed no significant decrease from polysaccharide coatings without added crosslinking reagent. (See appendix B, tubes 18 to 56).

The effect of silane coating followed by methylcellulose coating is observed in the following control experiments. The uncoated thick-walled capillaries (tubes 1, 2, and 3) had an average ΔEstr/ΔP of -0.357.

These three capillaries (1,2,3) were coated with γ-glycidoxypropyltrimethoxysilane/triethylamine; 1/1, and cured in vacuum at room temperature; the ΔEstr/ΔP dropped to -0.310 (tubes 57, 58 and 59). The tubes were then treated with methylcellulose in 0.5% HCl and then heated to 120° in vacuum overnight, the ΔEstr/ΔP average value fell to -0.083 (tubes 60, 61 and 62). To see if a further coating of methylcellulose would lower the streaming potential, the last three tubes were recoated with methylcellulose in 0.5% HCl containing 5% 1,2,4,5,9,10-triepoxydecane (25) as crosslinker, and then cured overnight at 120° in vacuum. The streaming potential increased slightly, with an average ΔEstr/ΔP of -0.103 (tubes 63, 64 and 65). These results are summarized in Table I below.

TABLE I

Tube Treatment	ΔEstr/ΔP
uncoated tube (tubes 1, 2, and 3)	-0.357
tube silanized with γ-glycidoxypropyltrimethoxysilane (not heated in oven) (tubes 57, 58, and 59)	-0.310
tube silanized as above, recoated with methyl cellulose in 0.5% HCl (heated in oven at 120°C overnight) (tubes 60, 61 and 62)	-0.083
methylcellulose coated tube above recoated with methylcellulose in 0.5% HCl containing 5% 1,2,4,5,9,10-triepoxydecane as crosslinker (tubes 63, 64, and 65)	-0.103

Six additional tubes (35-41) were treated with the epoxysilane as described above. This silane treatment was then followed by various polysaccharides in either 0.5% HCl or 0.5% KOH, finally curing the tubes at 120°C in vacuum. All base treated tubes (36, 38 and 41) had high ΔEstr/ΔP values. The tubes treated with either methylcellulose or hydroxypropylmethylcellulose in 0.5% HCl exhibited low ΔEstr/ΔP values (35 and 37). The effect of KOH on the streaming potential may not be surprising since strong base is known to etch glass surfaces.

To test if the high temperature - KOH coating procedure had an adverse effect, an epoxysilane-coated tube was recoated with methylcellulose in 0.5% KOH and then cured at 60° in vacuum overnight. Now the $\Delta Estr/\Delta P$ value (tube 52), (-0.087) was in the range that tubes treated with methylcellulose in 0.5% HCl exhibit. Still, the lowest streaming potential for polysaccharide treated tubes was obtained by first the epoxysilane treatment followed by methylcellulose in 0.5% HCl (tube 53, $\Delta Estr/\Delta P = -0.028$).

D. Effect of Hydrophilic Acrylate and Methacrylate Coatings

A coupling agent is required to covalently bond a methacrylate (acrylate) polymer to a glass surface. For this reason, the glass surface was first silanized with γ-methacryloxypropyltrimethoxysilane/triethylamine; 1/1. This silane treatment lowers the $\Delta Estr/\Delta P$ of the capillaries to a value typical of silanes in general. (Average $\Delta Estr/\Delta P = -0.197$, tubes (42, 43,44, 45). The monomers used in this study were hydroxyethyl methacrylate (26), methacrylic acid (27) acrylamide (17), and triethyleneglycol monomethacrylate (28).

A radical initiator was added to the monomer. 2,2-Azobis(methyl isobutyrate) (29) is routinely used in our laboratory to initiate radical polymerization (34). This compound has very similar decomposition rates to azobisisobutyronitrile (AIBN) but exhibits much better solubility properties in the hydrophilic monomers. In certain tubes the crosslinking agent, ethyleneglycol dimethacrylate (30), was added to the monomer.

The tubes were silanized and then heated to 120°C. They were removed from the oven while still hot. In these experiments the methacrylates were prepared as soluble solutions by radical initiaiton at low dilution (1 to 10, v/v) in ethanol (31), (32), (33). The capillary tube is then held in a vertical position and a small amount of the solution is allowed to flow through the tube. The tubes were cured overnight at 60°C and then re-equilibrated in distilled water. In this manner, very thin, uniform hydrogel coats were deposited on the inside of the capillary.

Capillary coatings of the following polymers were prepared and measured: poly(methoxyethyl methacrylate) (PMEMA), poly(hydroxyethyl methacrylate (PHEMA) and poly(methoxyethoxyethyl methacrylate) (pMEEMA). These polymers swell in water to incorporate 3.5%, 40% and 63% water, respectively (34). The ΔEstr/ΔP values for these polymers are comparable to the best values obtained for the methylcellulose coatings. The large difference in degree of hydration for these polymers showed no statistical difference in their streaming potential values as shown in Table II.

TABLE II

Coating	% Hydration	ΔEstr/ΔP	StD. Dev
poly(methoxyethyl methacrylate)	3.5	-0.058	0.050
poly(hydroxyethyl methacrylate)	40	-0.046	0.029
poly(methoxyethoxyethyl methacrylate	63	-0.038	0.012

E. Effect of Charge Group Incorporation into Hydrophilic Methacrylate Coatings

For this study hydroxyethyl methacrylate (HEMA) was selected as the fundamental monomer. Positive charge groups were incorporated into the polymer backbone by copolymerization of HEMA with dimethylaminoethyl methacrylate (DMAEMA). The copolymerization takes place in ethanol at high dilution (1/10, v/v). Since the DMAEMA exists as a uncharged species at the pH of the streaming fluid, 3 times molar excess of methyl iodide was added after polymerization. The methyl iodide functions to quaternize the free amine forming a quaternary ammonium salt (35).

Negative charge groups were incorporated into the HEMA polymer by copolymerization with methacrylic acid (MAA) in high dilution in ethanol (1/10, v/v). The MAA residue exists in its ionic form at the pH of the streaming fluid. The capillary tubes are coated as described for the hydrophilic methacrylate polymers. The results of the experiment are shown in Table III.

TABLE III

Coatings	$\Delta E_{str}/\Delta P$	StD. Dev
pHEMA	-0.046	0.029
pHEMA with 1% MAA	-0.080	0.024
pHEMA with 3% MAA	-0.100	0.024
pHEMA with 10% MAA	-0.113	0.035
pHEMA with quaternized 0.1% DMAEMA	-0.015	
pHEMA with quaternized 1% DMAEMA	+0.070	0.024
pHEMA with quaternized 3% DMAEMA	+0.074	0.004
pHEMA with quaternized 10% DMAEMA	0.087	0.014

Increased amounts of methacrylic acid in the polymer increases the streaming potential in a negative direction. Quaternized DMAEMA groups in the polymer decrease the streaming potential values giving essentially zero values at 0.1 mole % incorporation. Further increases in the amount of quaternized DMAEMA gives increasing positive streaming potential values. The streaming potential is not a linear function of the mole percent charge incorporated into the polymer but is highly affected by the first mole percent of charge and is less sensitive at higher charge incorporation. This is shown in figure 8.

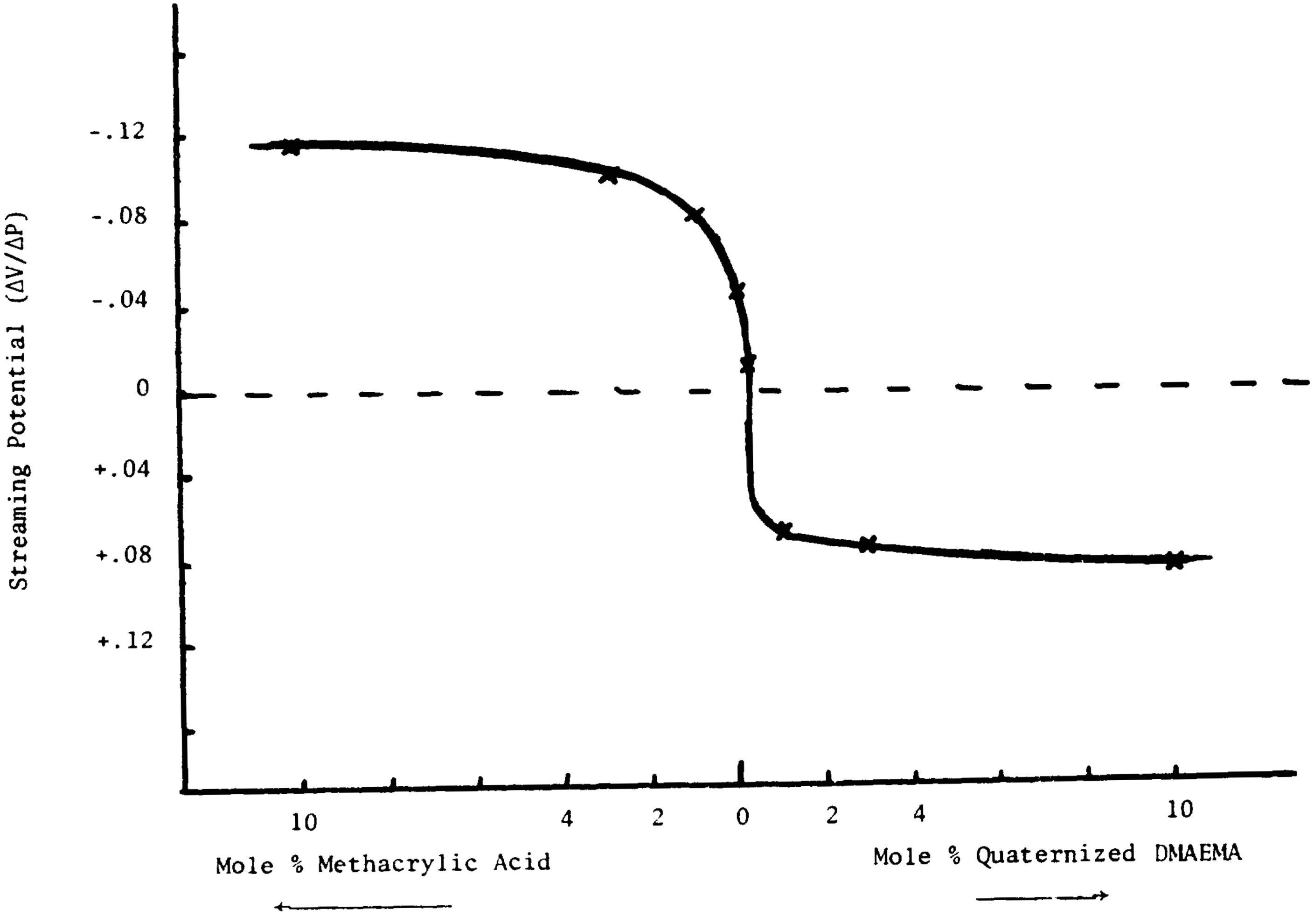

Figure 8. Streaming Potential of HEMA-coated capillaries as a function of type and amount of charged group.

V. CONCLUSIONS AND RECOMMENDATIONS

An apparatus and protocol is described for streaming potential determinations of capillary tubes. The streaming potential technique is very dependent on capillary size, ionic strength, electrode preparation, flow turbulence and pH as shown in part I of the text. Such effects had to be investigated to assure reliable, meaningful results.

The most important conclusions on the effect of various coatings on glass capillaries are:

1. All silanizing reagents gave similar ΔEstr/ΔP values, which is approximately half the value of the uncoated tubes.
2. γ-glycidoxypropyltrimethoxy silane treatment followed by methyl cellulose or hydroxypropylmethyl cellulose in 0.5% HCl gave consistantly the lowest ΔEstr/ΔP values. The γ-glycidoxypropyltrimethoxy silane/methylcellulose was used in the zero gravity cell electrophoresis experiment performed during the Appolo-Soyuz joint space flight, July 15, 1975. In this experiment, the cells gave good migration profiles.
3. Coating of hydrophilic methacrylate gels gave low streaming potential to values comparable to the γ-glycidoxypropyltrimethoxy silane/methylcellulose treatment. No statistical difference is noted in streaming potential values between gels of different equilibrium water content.
4. Charged groups incorporated into the hydrophilic methacrylate gels changed streaming potential values accordingly: negative charges increase streaming potential negatively. Positive charge has the opposite effect. Since the uncharged hydrophilic methacrylate gels exhibit slightly negative streaming

potential value, a very small amount of positive charge incorporation ($\sim$ 0.1 mole percent) gives a gel coating having essentially zero streaming potential.

REFERENCES

1. M. Helmholts, Wied. Ann., 1, 337, (1879), M. Smoluchowski, "Handbuch der Elektrizitat und des Magnetismus", Vol. 11, Graetz (ed.), p. 366, Burth, Leipzig (1921).
2. J. T. Davies and E. K. Rideal, "Interfacial Phenomena", 2nd ed., p. 108, Academic Press, New York (1963).
3. D. A. Haydon, Recent Prog. Surf. Sci., 1, 94 (1964).
4. B. Ball and D. W. Fuerstenau, Miner, Sci. Eng., 5, 267, (1973).
5. G. Jones and B. C. Bradshaw, J. Am. Chem. Soc., 55, 1780 (1933).
6. P. E. Bocquet, Ph.D. Thesis, University of Michigan (1952).
7. L. Prandtl and O. G. Tietjens, "Applied Hydro- and Aeromechanics", p. 22, McGraw-Hill, New York.
8. H. L. Langhaar, Trans. Am. Soc. Mech. Eng., 64, A55 (1942).
9. R. Van Wagenen, Ph.D. Dissertation, University of Utah, in preparation.
10. G. T. Janz and D. J. C. Ives, Ann. N. Y. Acad. Sci., 148, 210 (1968).
11. S. Srinivasan, Brookhaven National Labs, Upton, L. I., N. Y., 11973, personal communication.
12. M. L. Hair and W. J. Hertl, J. Phys. Chem., 74, 91, (1970).
13. K. Marshall, G. L. Ridgewell, C. H. Rochester and J. Simpson, Chem. Ind. (London), 19, 775 (1974).
14. F. M. Ernsberger, Annu. Rev. Mater. Sci., 2, 529 (1972).
15. A. J. Rutgers and M. De Smet, Trans. Faraday Soc., 43, 102 (1947).
16. H. C. Li and P. L. De Bruyn, Surf. Sci., 5, 203 (1966).
17. Obtained from Eastman Kodak Company, Rochester, N. Y.
18. I. V. Borisenko, A. V. Kiselev, R. S. Petrova, U. K. Chuikima and K. D. Shcherbakova, Russ. J. Phys. Chem., 39, 1436 (1965).
19. Obtained from Marshallton Research Laboratories, West Chester, Pennsylvania 19380.
20. "Interaction of Alkoxy Silane Coupling Agents", R. L. Kaas and J. L. Kardos, Monsanto Research Corporation Report (1970), St. Louis, Missouri 63166.

21. "Silane Coupling Agents" Dow Corning Research Bulletin, (1970), Midland, Michigan 48640.

22. Obtained from Matheson, Coleman and Bell, East Rutherford, N. J.

23. Obtained from Stein, Hall and Company, New York, N. Y.

24. Obtained from Bio-Rad Laboratories, Richmond, California.

25. Obtained from Alfred Bader Company, Division of Aldrich Chemical Company, Milwaukee, Wisconsin 53210.

26. Obtained from Hydro Med Sciences, Inc., New Brunswick, N. Y. 08902.

27. Obtained from Rohm and Haas, Philadelphia, Pennsylvania 19105.

28. This compound was a research sample from our lab.

29. Prepared by the method of G. A. Mortimer, J. Org. Chem., 30, 1632 (1965).

30. Obtained from Monomer-Polymer Laboratories, Philadelphia, Pennsylvania 19124.

31. M. Bohdanecky and Z. Tuzar, Coll. Czech. Chem. Comm., 34, 3318 (1969).

32. K. Dusek, Coll. Czech. Chem. Comm., 34, 3309 (1969).

33. M. Bohdanecky, Z. Tuzar, M. Stoll and R. Chromecck, Coll. Czech. Chem. Comm., 33, 4104 (1968).

34. D. E. Gregonis, C. M. Chen and J. D. Andrade, in "Hydrogels for Biomedical and Related Applications", J. D. Andrade, ed. ACS Symposium Series, 1976, in press.

35. M. A. Korshunov. F. N. Bondariuk, V. E. Lazaryants, A. M. Kutin, K. N. Malkova and N. A. Prebrezhansky, British Pat. 1,177,227 (1970).

APPENDIX A

in Hydrogels for Medical and Related Applications, J. D. Andrade, ed.,
American Chemical Society Symp. Series, in press, 1976.

STREAMING POTENTIAL STUDIES ON GEL-COATED GLASS CAPILLARIES

Shao M. Ma, Donald E. Gregonis, Richard Van Wagenen
Joseph D. Andrade
Department of Materials Science & Engineering
University of Utah
Salt Lake City, Utah 84112

The separation of living cells in zero gravity environments appears to offer significant advantages over analogous separations on earth. The zero gravity environment eliminates sedimentation and density fluctuation problems. As demonstrated in Apollo 16 experiments (1), a major problem with free zone electrophoresis in a closed system is the differential fluid movement due to the surface electrical properties of the container (electroosmosis). As a consequence, the resolution of the separation and the analysis involved are grossly compromised by the resulting "bullet" shape flow patterns. A solution to this problem is to produce surfaces which exhibit essentially no electrokinetic properties when in equilibrium with their environment. This can be achieved by neutralizing the surface charge or by shifting the hydrodynamic shear plane away from the interface by use of hydrophilic surface coatings.

In this study, glass tubes were subjected to various coatings and surface treatments. In particular, it was felt that uncharged hydrophilic methacrylate polymer coatings should decrease the electroosmosis. The overall effects of these treatments upon streaming potential is discussed.

Apparatus

The streaming potential apparatus has been described in detail (2,3). It is an all-glass system utilizing Ag/AgCl electrodes. Streaming fluid is forced back and forth from one reservoir to the other through a glass tube using pressurized pure nitrogen gas. A glass pH electrode and a thermometer are positioned in one of the reservoirs. A Keithley model 616 digital electrometer measures streaming potential or streaming current.

All new and large glassware are cleaned initially in chromic sulfuric acid, thoroughly rinsed in running, distilled water, soaked in doubly distilled water, rerinsed in double distilled water and then air dried in a dust-free environment. Small glassware is cleaned by radiofrequency glow discharge (4).

To carry out the streaming potential measurement each reservoir is filled with about 500 ml of phosphate buffer at pH 7.2 containing 0.01 M KCl. The electrodes are inserted. The potential is then measured as a function of driving pressure. The streaming potential, E_{str}, is linearly dependent on the pressure drop, P, across the tube, as given by (5)

$$\zeta = \frac{4\pi\eta K}{D} \frac{E_{str}}{P}$$

where ζ is the zeta potential, η and D are the viscosity and dielectric constant, respectively, in the diffuse portion of the electrical double layer, and K is the bulk specific conductivity of the electrolyte (assuming surface conductance is negligible relative to bulk conductance).

Ball and Fuerstenau (6) have reviewed the streaming potential literature in regard to streaming potential data. They have concluded that, due to as yet unexplained flow and symmetry potentials common to a wide variety of electrode types, the slope of the loci of E_{str} data at a number of driving pressures, P, in opposite flow directions, $\Delta E_{str}/\Delta P$, should be utilized in the above equation. This has been the case in this study. Streaming potential data was obtained by measuring streaming potentials at a driving pressure of 2cm Hg, then reversing the flow direction and repeating the measurement. The driving pressure was increased by 2cm Hg and streaming potentials were again measured in both flow directions. This process was repeated until the driving pressure reached 12cm Hg. The loci of streaming potential data as a function of driving pressure were then fitted to a linear regression best fit straight line using a Hewlett Packard (Model 9820A) programmable calculator.

Absolute values of zeta potential calculated from the above equation may be erroneous due to assumptions concerning values for double layer viscosity, dielectric constant, and entrance flow effects resulting from the large ID of the tubes utilized in this study (2,3).

Materials

Thick-walled "Pyrex" capillary tubes, approximately 0.2cm ID and 15cm long, were used. Uncoated capillaries had $\Delta E_{str}/\Delta P$ of -0.357 mV/cm Hg.

Different silane adhesion promoters (7) were used to pretreat the glass surfaces prior to gel coating. An investigation of several silanizing reagents using different procedures showed a slight decrease in $\Delta E_{str}/\Delta P$ for all the silane coatings. The $\Delta E_{str}/\Delta P$ values were not sensitive to the organic functionality of the silane.

A variety of hydrophilic polymers were used as coating materials including methylcellulose (Dow Methocel MC, premium, 4000 cps); hydroxypropylmethylcellulose (Dow Methocel, 90Hg, premium, 15000 cps); dextrin (Matheson, Coleman and Bell) and agarose (Biorad Labs). Hydroxyethyl methacrylate was donated by Hydro Med Sciences, Inc. Methoxyethyl methacrylate and methoxyethoxyethyl methacrylate were prepared in our laboratories by base catalyzed transesterification of methyl methacrylate with the corresponding alcohol (8).

Methods and Results

The silane compounds were applied using standard procedures (6). A silane solution was rinsed through the tubes, first in one direction, then in the other, and the tubes were vacuum dried overnight. The silane compounds used and the $\Delta E_{str}/\Delta P$ values are given in Table I.

TABLE I.

$\Delta E_{str}/\Delta P$ Values for Silane Coatings

Coating	$\Delta E_{str}/\Delta P$ (mV/cm Hg)
1,1,1,3,3,3-hexamethyldisilazine:triethylamine	-0.242
Chlorotrimethylsilane:triethylamine (1:1)	-0.221
Dichlorodimethylsilane:triethylamine (1:1)	-0.253
γ-methacryloxypropyltrimethoxysilane:triethylamine (1:1)	-0.234
γ-glycidoxypropyltrimethoxysilane:triethylamine (1:1)	-0.229
γ-glycidoxypropyltrimethoxysilane:n-propylamine (1:1)	-0.230
γ-glycidoxypropyltrimethoxysilane:pH 4 aq. acetic acid	-0.241

The γ-glycidoxypropyltrimethoxysilane:triethylamine (1:1) silane coating was selected for further treatment with the neutral polysaccharides. It was thought that coating the polysaccharides upon the epoxy-silanized glass was either an acid or base catalyzed process resulting in covalent attachment of the polysaccharide to the surface (Figure 1).

Standard solutions of various polysaccharides were prepared by dissolving in either 0.5% HCl or 0.5% KOH. If the polysaccharide was soluble, the viscosity of the solution was "regulated" by the addition of polysaccharide until it had the consistency of a thick syrup. Otherwise the polysaccharide was added to complete saturation. The polysaccharide solution was pulled through the tubes in each direction by a water-aspirator partial vacuum. The tubes were then placed in a vacuum oven at 120°C for 12 hours, unless otherwise specified. The tubes were exhaustively rinsed with distilled water and the $\Delta E_{str}/\Delta P$ values were obtained.

Consistently lower $\Delta E_{str}/\Delta P$ values were obtained when the polysaccharides were applied in acidic solution as compared to basic solution; however, when methylcellulose in distilled water was applied to the epoxy-silanized glass, a $\Delta E_{str}/\Delta P$ value was obtained comparable to the results obtained with methylcellulose in acid solution. At the moment the mechanism that governs attachment of methylcellulose to the epoxy-silanized glass is in doubt. The treatment of glass surfaces with just methylcellulose or γ-glycidoxypropyltrimethoxysilane does not give the low $\Delta E_{str}/\Delta P$ values. This phenomenon is still being investigated.

Further coating of methylcellulose onto a methylcellulose coating showed no change in $\Delta E_{str}/\Delta P$. The use of 1,2,4,5,9,10-triepoxydecane (TED) as a crosslinker in the methylcellulose solutions (5% TED in 0.5% HCl-methylcellulose) was investigated. Curing was accomplished by heating overnight at 120°C in vacuum. No statistical change was noted for this treatment over normal methylcellulose tubes (Table II).

TABLE II.

Effects of Silane and Polysaccharide Coatings Upon $\Delta E_{str}/\Delta P$ Values

Coating	$\Delta E_{str}/\Delta P$ (mV/cm Hg)	Standard Deviation
(1) Uncoated	-0.356	0.010
(2) γ-glycidoxypropyltrimethoxysilane:triethylamine (1:1)	-0.310	0.007
(3) Procedure 2, then 0.5% HCl	-0.226	---
(4) Procedure 2, then 0.5% KOH	-0.261	---
(5) Methylcellulose in distilled H_2O	-0.166	0.090
(6) Procedure 2, then methylcellulose in 0.5% KOH	-0.130	0.012
(7) Procedure 2, then methylcellulose in 0.5% HCl	-0.078	0.008
(8) Procedure 2, then methylcellulose in distilled H_2O	-0.058	0.002
(9) Methylcellulose coated tubes (Procedure 7) recoated with methylcellulose with 5% 1,2,4,5,9,10-triepoxydecane on 0.5% HCl	-0.103	0.003
(10) Procedure 2, then hydroxypropylmethylcellulose in 0.5% HCl	-0.096	---
(11) Procedure 2, then dextrin in 0.5% HCl	-0.245	---
(12) Procedure 2, then agarose in 0.5% HCl	-0.250	---

A simple water-polyfluorocarbon surface contact angle test was used to detect surface-active extractables (9) from the coated capillaries. High contact angles were noted with all tubes. No significant change in the contact angle was evident with the methylcellulose-coated tubes, indicating that the methylcellulose is not readily extracted from the surface.

To obtain capillary tubes coated with methacrylate hydrogels, first soluble polymers were prepared. This was accomplished by radical initiation of the desired monomer at low dilution (1 to 10, v/v) in ethanol. A small amount of this polymer solution is allowed to flow through the glass capillary, and with a little care and patience, a very uniform coat of the polymer could be deposited on the inside of the capillary.The viscosity of the polymer solution was regulated by the addition or evaporation of solvent. The tubes were cured overnight at 60°C and then allowed to equilibrate in distilled water.

The monomers that were investigated were methoxyethyl methacrylate (MEMA), hydroxyethyl methacrylate (HEMA) and methoxyethoxyethyl methacrylate (MEEMA). It has been determined that these polymers swell in water to incorporate 3.5%, 40% and 63% water, respectively (9). The corresponding $\Delta E_{str}/\Delta P$ values are comparable to the best methylcellulose values (Table III).

TABLE III.

Effects of Hydrophilic Methacrylate Coatings Upon $\Delta E_{str}/\Delta P$ Values

	Coating	$\Delta E_{str}/\Delta P$ (mV/cm Hg)	Standard Deviation
(1)	Uncoated tubes	-0.290	0.045
(2)	Hydroxyethyl methacrylate (HEMA)	-0.046	0.029
(3)	Methoxyethyl methacrylate (MEMA)	-0.058	0.050
(4)	Methoxyethoxyethyl methacrylate (MEEMA)	-0.038	0.012
(5)	HEMA with 1% methacrylic acid (MAA)	-0.080	0.024
(6)	HEMA with 3% MAA	-0.100	0.024
(7)	HEMA with 10% MAA	-0.113	0.035
(8)	HEMA with quaternized 1% dimethylaminoethyl methacrylate (DMAEMA)	+0.070	0.024
(9)	HEMA with quaternized 3% DMAEMA	+0.074	0.004
(10)	HEMA with quaternized 10% DMAEMA	+0.087	0.014

To observe the effect that charged groups in the hydrophilic polymers had upon $\Delta E_{str}/\Delta P$ values, HEMA was polymerized at low dilution with various amounts of methacrylic acid (MAA) and dimethylaminoethyl methacrylate (DMAEMA).

In the streaming solution buffered to pH 7.2, methacrylic acid exists as the charged salt, but dimethylaminoethyl methacrylate exists as an uncharged species. After polymerization of the HEMA-DMAEMA copolymer, methyl iodide was added to the polymer solution to react with the free amino groups forming quaternary ammonium iodides (Figure 2). The capillary tubes were coated as described for the other methacrylate polymers, cured at 60°C overnight and then allowed to swell to equilibrium in either distilled water or streaming potential buffer.

The MAA-HEMA copolymer coatings exhibited average $\Delta E_{str}/\Delta P$ values which increased negatively with increasing percentage of methacrylic acid in the polymer: -0.080 for 1% MAA, -0.100 for 3% MAA, and -0.113 for 10% MAA. The quarternary DMAEMA-HEMA copolymer coatings produced a net positive electrokinetic surface as indicated by increasingly positive $\Delta E_{str}/\Delta P$ values with increasing percentage of DMAEMA; +0.070 for 1% DMAEMA, +0.074 for 3% DMAEMA, and +0.087 for 10% DMAEMA (Table III).

Discussion

According to Brook's model (10) the zeta potential in the presence of adsorbed polymer (hydrophilic, uncharged) could be higher or lower than that in the absence of polymer. The effect depends on the relative magnitude of the thickness of the adsorbed polymer layer, d, and the thickness, d_f, within which nonzero fluid flow occurs during an electrokinetic experiment. Three areas have been cited:

1. For a totally free draining adsorbed layer, the location of the shear plane is unaffected by the presence of the adsorbed layer, i.e. $d = d_f$. In this case, polymer adsorption causes an increase in zeta potential.
2. For a partially free draining adsorbed layer, the shear plane is shifted to a position within the adsorbed polymer layer ($0 < d_f < d$). In this case polymer adsorption may cause either an increase or a decrease in zeta potential.
3. When flow is totally excluded from the adsorbed layer, i.e., the shear plane is shifted outside the adsorbed layer ($d_f = 0$,, polymer adsorption causes a decrease in zeta potential.

Our data was obtained from a large variety of neutral polymer coatings; all show a decrease in $\Delta E_{str}/\Delta P$. Our neutral polymer coatings were cast on glass capillary surfaces and are thicker than those obtained by adsorption. Although one cannot directly compare our coatings with the three cases presented by

Brook's (10) it does appear that in our case the shear plane has been shifted far away from the interface. Consider the $\Delta E_{str}/\Delta P$ values given in Table III for positive or negative groups copolymerized with HEMA. At low streaming potential values, increased experimental error is introduced into the measurements. At a given P, E_{str} changes with time, partly due to a change in the relative fluid levels in the two reservoirs which causes a change in P and partly due to electrode drift with time of unknown cause (2-3). It was observed that the ΔE_{str} readings were more stable for surfaces with high streaming potentials. As a consequence, the error is larger when the absolute $\Delta E_{str}/\Delta P$ value is small. Although different samples of similar coating or the same sample measured on different days do show large variations in their $\Delta E_{str}/\Delta P$ values, when the same sample was measured three times within a short period, its $\Delta E_{str}/\Delta P$ value was quite consistent. Also, in each series of measurements, the $\Delta E_{str}/\Delta P$ value for samples 5-10 followed the same trend as given in Table III. Therefore, we would like to attribute the large standard deviation values to the variations in experimental conditions, surface roughness, uneven coatings, etc., and consider the effect of increasing absolute streaming potential values with increasing charge as real.

Conclusions

A decrease in $\Delta E_{str}/\Delta P$ occurs when the glass surface is silanized or coated with a neutral polysaccharide such as methylcellulose. Silanization followed by methylcellulose treatment gives an almost ten-fold decrease in $\Delta E_{str}/\Delta P$ over uncoated "Pyrex" glass. Both acid and neutral methylcellulose solutions coated upon a γ-glycidoxypropyltrimethoxysilane base gives the lowest $\Delta E_{str}/\Delta P$ values for the polysaccharides examined. Base-containing methylcellulose deposited on a γ-glycidoxypropyltrimethoxysilane surface gives slightly higher $\Delta E_{str}/\Delta P$ values, perhaps due to the corrosive action of the base. No additional improvement in $\Delta E_{str}/\Delta P$ values was obtained when the methylcellulose tubes are recoated with methylcellulose containing a crosslinker.

Hydrophilic methacrylate polymer coatings also lower $\Delta E_{str}/\Delta P$ values about ten-fold over untreated glass capillaries. By added quaternary ammonium groups to these polymer coatings, the sign of $\Delta E_{str}/\Delta P$ is changed from negative to positive. It is felt that by adjusting the amount of charged co-monomers, a zero $\Delta E_{str}/\Delta P$ value could be obtained.

Aeronautics and Space Administration, Marshall Space Flight Center, Huntsville, Alabama, under Contract No. 8-30253, Dr. J. Patterson, Contract Monitor. The assistance of R. Middaugh is gratefully acknowledged.

Abstract

Streaming potential techniques were used to measure the interfacial electrical potential of glass capillaries. Different silanizing reagents were used to coat the glass capillaries and decrease the streaming potential values by a comparable amount, i.e., about half that of the uncoated glass capillaries. A ten-fold decrease in streaming potential is observed when methylcellulose is coated onto a γ-glycidoxypropyl silanized glass capillary. A comparable decrease is noted when hydroxyethyl methacrylate (HEMA), methoxyethyl methacrylate (MEMA) and methoxyethoxyethyl methacrylate (MEEMA) polymers are coated on the glass capillary. By adding anionic or cationic charged groups to the poly-HEMA coating, streaming potential values of opposite sign are obtained.

Increasing the amount of methacrylic acid copolymerized with the HEMA monomer negatively increases the average $\Delta E_{str}/\Delta P$ values. Increasing the amount of quaternized dimethylaminoethyl methacrylate in the copolymer positively increases the average $\Delta E_{str}/\Delta P$ values.

Literature Cited

1. Snyder, R. S., Bier, M., Griffin, R. N., Johnson, A. J., Leidheiser, Jr., H., Micale, F. J., Vanderhoff, J. W., Ross, S., van Oss, C. J., Sep. Purific. Methods (1973) 2 (2), 259.
2. Van Wagenen, R., Ph.D. Dissertation, University of Utah, September 1975.
3. Van Wagenen, R., Andrade, J. D., and Hibbs, J. B., Jr., Submitted to J. Electrochem. Soc.
4. Hollahan, J. R., and Bell, A. T., Eds., "Techniques and Applications of Plasma Chemistry," Wiley, New York, 1974.
5. Davies, J. T., and Rideal, E. K., "Interfacial Phenomena," 2nd Ed., Academic Press, 1963.
6. Ball, B., and Fuerstenau, D. W., Miner. Sci. Eng., (1973) 5, 267.
7. Bascom, W. D., Macromolecules (1972) 5, 792.
8. Gregonis, D. E., Chen, C. M., and Andrade, J. D., "The Chemistry of Some Selected Methacrylate Hydrogels," this symposium.
9. Baier, R. E., Gott, V. L., and Feruse, A., Trans. Amer. Soc. Artificial Internal Organs (1970) 16, 50.
10. Brooks, D. E., J. Colloid and Interface Science, (1973) 43, 687.

a. Acid Catalyzed Process

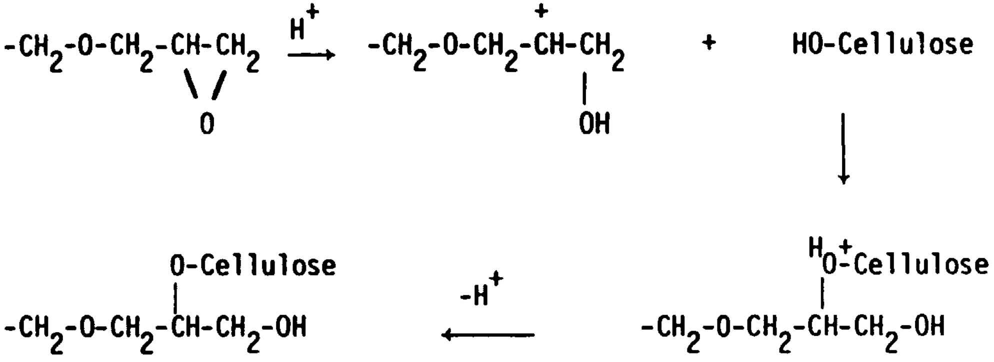

b. Base Catalyzed Process

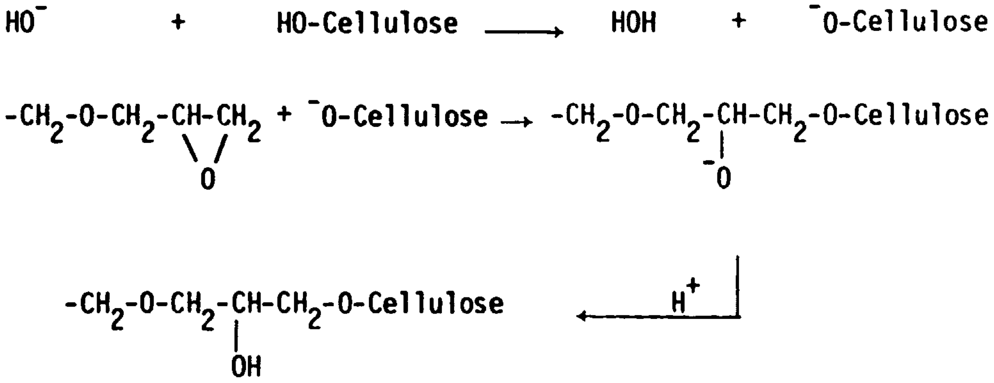

Figure 1. Reaction schemes for the attachment of polysaccharides to epoxy-silane surfaces: a) acid catalyzed; and b) base catalyzed.

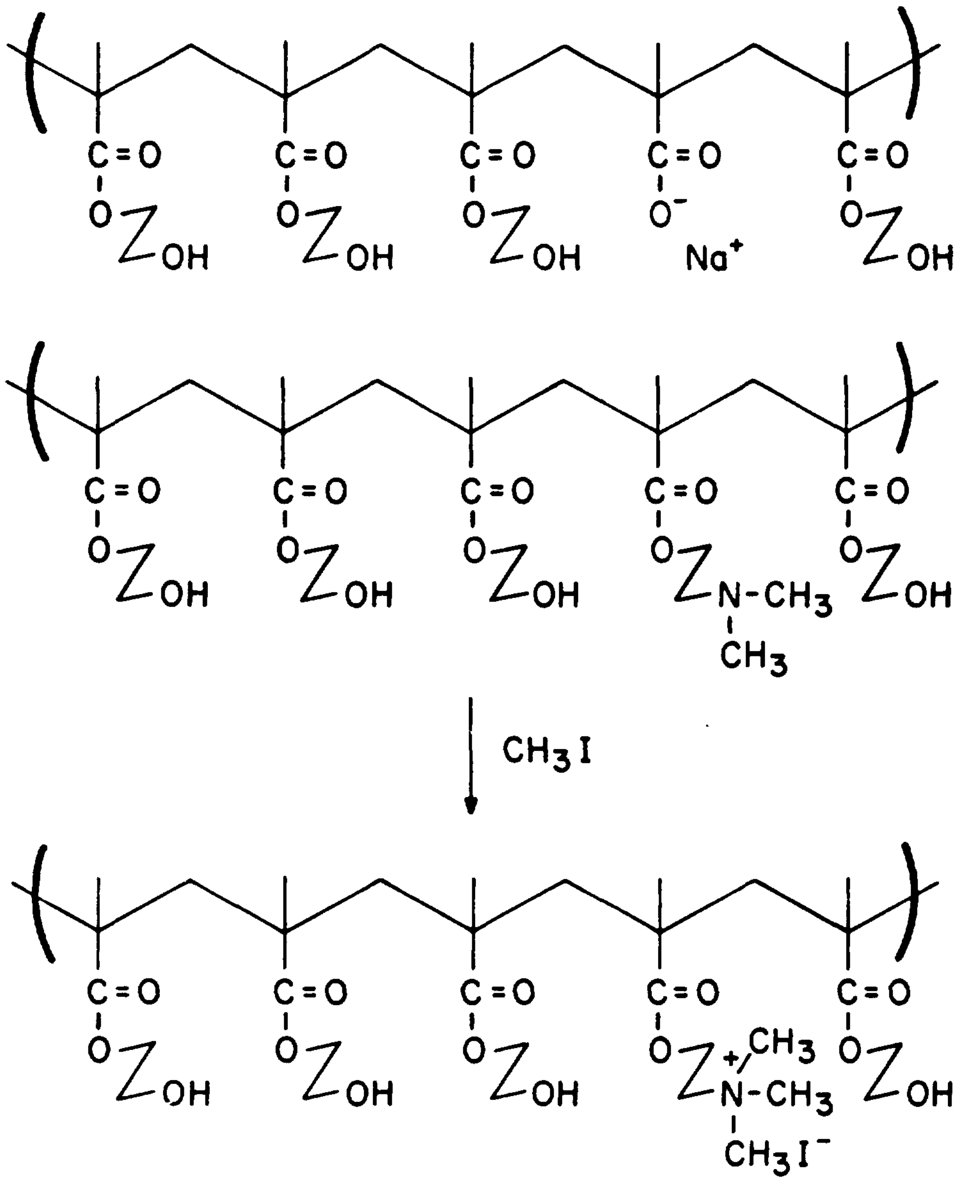

MAA - HEMA
COPOLYMER

DMAEMA - HEMA
COPOLYMER

QUATERNIZED DMAEMA
HEMA COPOLYMER

F. 2

APPENDIX B: COMPLETE TABLE OF ΔEstr/ΔP VALUES

Tube #	ΔEstr/ΔP		Treatment
1	-0.352	-0.357	Uncoated tube
2	-0.368		"
3	-0.351		"
4	-0.259	-0.242	Tube treated with 1,1,1,3,3,3-hexamethyldisilazine/triethylamine; 1/1.
5	-0.219		"
6	-0.239		"
7	-0.252		"
8	-0.259	-0.221	Tube treated with chlorotrimethylsilane/triethylamine; 1/1.
9	-0.181		"
10	-0.163		"
11	-0.282		"
12	-0.253		Tube treated with dichlordimethylsilane/triethylamine; 1/1.
13	-0.234		Tube treated with γ-methacryloxypropyltrimethoxysilane/triethylamine: 1/1.
14	-0.128		Tube treated with γ-glycidoxypropyltrimethoxysilane/triethylamine; 1/1.
15	-0.229		"
16	-0.230		Tube treated with γ-glycidoxypropyltrimethoxysilane n-propylamine: 1/1.
17	-0.241		Tube treated with γ-glycidoxypropyltrimethoxysilane pH. 4 aq. acidic acid: 1/1.
18	-0.230		Tube treated as #14, then methylcellulose in 0.5% KOH.
19	-0.055		Tube treated as #14, then methylcellulose in 0.5% HCl.

Appendix B (cont.)

Tube #	ΔEstr/ΔP	Treatment
20	-0.248	Tube treated as #14, then hydroxypropylmethylcellulose in 0.5% KOH.
21	-0.148	Tube treated as #14, then agarose in 0.5% KOH
22	-0.084	Tube treated as #14, then dextrin in 0.5% KOH
23	-0.199	Tube treated as #19, resilanized as tube 14, followed as methylcellulose in 0.5% KOH.
24	-0.049	Tube treated as #19, retreated with methylcellulose in 0.5% formaldehyde in 0.5% HCl.
25	-0.061	"
26	-0.055	Tube treated as #19, retreated with hydroxypropylmethylcellulose in 5% formaldehyde -0.5% HCl.
27	-0.104	Tube treated as #19, retreated with JAGUAR in 5% formaldehyde - 0.5% HCl
28	-0.046	Tube treated as #19, retreated with hydroxypropylmethylcellulose in 1,2,4,5,9,10-triepoxydecane - 0.5% HCl.
29	-0.037	Tube treated as #19, retreated with methylcellulose in 5% 1,2,4,5,9,10-triepoxydecane - 0.5% HCl.
30	-0.039	Tube treated as #19, retreated with JAGUAR in 5% 1,2,4,5,9,10-triepoxydecane in 0.5% HCl.
31	-0.200	Same as tube 22
32	-0.150	Tube treated with γ-glycidoxypropyltrimethoxysilane/triethylamine: 1/1.
33	-0.226	Tube treated as #32, then rinsed with 0.5% HCl
34	-0.261	Tube treated as #32, then rinsed with 0.5% KOH
35	-0.096	Tube treated as #32, then methylcellulose in 0.5% HCl
36	-0.240	Tube treated as #32, then methylcellulose in 0.5% KOH

Appendix B (cont.)

Tube #	ΔEstr/ΔP	Treatment
37	-0.096	Tube treated as #32, then hydroxypropylmethylcellulose in 0.5% HCl
38	-0.270	Tube treated as #32, then hydroxypropylmethylcellulose in 0.5% KOH
39	-0.245	Tube treated as #32, then dextrin in 0.5% HCl
40	-0.250	Tube treated as #32, then agarose in 0.5% HCl
41	-0.284	Tube treated as #32, then agarose in 0.5% KOH
42	-0.195	Tube treated with γ-methacryloxypropyltrimethoxysilane/triethylamine: 1/1.
43	-0.148	"
44	-0.252	Treated as tube 42, followed with HEMA containing 0.2% azobis(methyl isobutyrate)
45	-0.237	"
46	-0.222	Treated as tube 44, followed by recoating of HEMA containing 6% azobis(methyl isobutyrate)
47	-0.220	"
48	-0.192	Treated as tube 42, followed by methacrylic acid with 5% ethylene glycol dimethacrylate containing 2.5% azobis(methyl isobutyrate)
49	-0.043	Treated as tube 42, followed by acrylamide/ H_2O with 5% ethylene glycol dimethacrylate containing 2.5% azobis(methyl isobutyrate)
50	-0.187	Treated as tube 42, followed by HEMA with 5% ethylene glycol dimethacrylate, 2.5% azobis(methyl isobutyrate)
51	-0.229	Treated as tube 42, followed by triethylene glycol monomethacrylate with 5% ethylene glycol dimethacrylate, 2.5% azobis(methyl isobutyrate)
52	-0.087	Treated as tube 32, followed by methylcellulose in 0.5% KOH, heated at 60°C for 12 hours

Appendix B (cont.)

Tube #	ΔEstr/ΔP		Treatment
53	-0.028		Treated as tube 32, followed by methylcellulose in 0.5% HCl
54	-0.053		Treated as tube 32
55	-0.040		Treated as tube 32, followed by agarose in 0.5% HCl
56	-0.115		Methylcellulose with 5% - 1,2,4,5,9,10-triepoxydecane in 0.5% HCl
57	-0.304	-0.310	Tube 1 treated with γ-glycidoxypropyltrimethoxysilane/triethylamine: 1/1 (not heated in oven)
58	-0.317		Tube 2 treated as tube 57
59	-0.308		Tube 3 treated as tube 57
60	-0.078	-0.083	Tube 57 treated with methylcellulose in 0.5% HCl
61	-0.093		Tube 58 treated with methylcellulose in 0.5% HCl
62	-0.077		Tube 59 treated with methylcellulose in 0.5% HCl
63	-0.100	-0.103	Tube 60 treated with methylcellulose with 5% 1,2,4,5,9,10-triepoxydecane in 0.5% HCl
64	-0.106		Tube 61 treated with methylcellulose with 5% 1,2,4,5,9,10-triepoxydecane in 0.5% HCl
65	-0.102		Tube 62 treated with methylcellulose with 5% 1,2,4,5,9,10-triepoxydecane in 0.5% HCl
66	-0.268	-0.271	Uncoated tube
67	-0.282		"
68	-0.262		"
69	-0.066	-0.046	Tube coated with soluble PHEMA
70	-0.079		"
71	-0.071		"
72	-0.012		"

Appendix B (cont.)

Tube #	ΔEstr/ΔP		Treatment
73	-0.027	-0.046	"
74	-0.023		"
75	-0.039	-0.066	Tube coated with soluble PMEMA
76	-0.044		"
77	-0.115		"
78	-0.032	-0.028	Tube coated with soluble PMEEMA
79	-0.026		"
80	-0.028		"
81	-0.064	-0.080	Tube coated with soluble PHEMA containing 1% MAA
82	-0.119		"
83	-0.051		"
84	-0.086		"
85	-0.074		"
86	-0.085		"
87	-0.131	-0.100	Tube coated with soluble PHEMA containing 3% MAA
88	-0.118		"
89	-0.114		"
90	-0.086		"
91	-0.078		"
92	-0.074		"
93	-0.120	-0.113	Tube coated with soluble PHEMA containing 10% MAA
94	-0.129		"
95	-0.172		"
96	-0.075		"
97	-0.087		"
98	-0.097		"

Appendix B (cont.)

Tube #	ΔEstr/ΔP		Treatment
99	-0.013		Tube coated with soluble PHEMA containing 0.1% quaternized DMAEMA
100	-0.018	-0.014	"
101	-0.011		"
102	+0.109		Tube coated with soluble PHEMA containing 1% quaternized DMAEMA
103	+0.049		"
104	+0.041	+0.069	"
105	+0.069		"
106	+0.074		"
107	+0.072		"
108	+0.072		Tube coated with soluble PHEMA containing 3% quaternized DMAEMA
109	+0.071		"
110	+0.074	+0.074	"
111	+0.079		"
112	+0.085		Tube coated with soluble PHEMA containing 10% quaternized DMAEMA
113	+0.076		"
114	+0.069	+0.087	"
115	+0.087		"
116	+0.097		"
117	+0.108		"